

# Comparison of defects produced by fast neutrons and $^{60}\text{Co}$ -gammas in high-resistivity silicon detectors using deep-level transient spectroscopy<sup>☆</sup>

M. Moll\*, H. Feick, E. Fretwurst, G. Lindström, C. Schütze

*II. Institut für Experimentalphysik, Universität Hamburg, Luruper Chaussee 149, D-22761 Hamburg, Germany*

## Abstract

Measurements of radiation-induced defects in high-resistivity silicon detectors irradiated with 14.1 MeV neutrons and  $^{60}\text{Co}$ -gammas have been performed using the Deep-Level Transient Spectroscopy technique (DLTS). Five electron traps and one hole trap were found in both neutron- and gamma-irradiated samples differing only in the relative defect concentrations. Furthermore, two additional levels were only detected in the neutron irradiated detectors. The observed defects are identified by comparing the measured energy levels, capture cross sections, and introduction rates to those known from literature. In addition, these assignments are supported by the annealing behaviour observed in two neutron-irradiated samples during a short-term annealing at room temperature and an isochronal heat treatment. The differences found between the defect production by fast neutrons and  $^{60}\text{Co}$ -gammas are discussed.

## 1. Introduction

In recent years extensive investigations on the radiation-induced changes of silicon detector properties have been performed leading to a particle- and fluence-dependent parametrisation of the macroscopic properties such as the effective doping concentration, the reverse current and the charge collection efficiency. Nowadays these parametrisations allow detailed predictions for the long term operability of silicon detectors for future applications in large colliders [1,2] but there is still considerable lack of understanding concerning the underlying microscopic defects. Although some models have been proposed connecting microscopic defect features with macroscopic detector properties [3,4], the defects fitting the model assumptions have up to now not been experimentally verified. One reason for this yet insufficient knowledge may be that most of the available spectroscopic data on defects in silicon pertain to electron-irradiated low-resistivity material while few such experiments have been made on hadron-irradiated high-resistivity material. In order to get more insight into the

microscopic processes that occur in detector grade silicon during and after hadron-irradiation the DLTS method was used in this work on neutron-irradiated detectors. Furthermore, a comparison to defects produced by gammas in detectors made from the same wafer reveals the peculiarities of neutron irradiation which in contrast to gamma respectively electron irradiation produces not only point defects but also clusters. Also the assignment of defect levels is aided by this comparison since many data exist on gamma- or electron-irradiated devices in the literature.

## 2. Experimental procedure

The samples are ion-implanted diodes with an active area of  $0.25\text{ cm}^2$  fabricated by the MPI-Halbleiterlabor München [5] from **n-type float zone silicon** (Wacker Chemitronic) with an initial resistivity of **3 k $\Omega$  cm**. The neutron irradiations were performed at the University Hospital Hamburg (UKE) with 14.1 MeV monoenergetic neutrons using the  $^3\text{H}(\text{d}, \text{n})^4\text{He}$  reaction [6]. All fluences given in this report are normalised to 1 MeV equivalent neutrons using the hardness factor of 1.88 taken from Ref. [7]. The average neutron flux was about  $1 \times 10^8\text{ n/cm}^2\text{ s}$ . The  $^{60}\text{Co}$ -gamma irradiations were carried out at the Brookhaven National Laboratory (BNL)

<sup>☆</sup> Work supported by the BMFT under contract 056HH17P.

\* Corresponding author. moll@sesam.desy.de.

with a dose rate of 150 krad per hour. During all irradiations the temperature was kept below 30°C. In total 7 samples were irradiated with neutrons in a fluence range from 1 to  $10 \times 10^{11}$  n/cm<sup>2</sup> and 4 with gammas in the dose range from 150 krad to 11 Mrad. The measurements of the defect levels were performed using a commercially available DLTS-apparatus [8]. The features of this system were previously outlined in Ref. [9] and are described in detail in Ref. [10]. Ionisation energies  $\Delta E_t$  and cross sections  $\sigma_t$  were obtained from Arrhenius plots. The defect concentrations  $N_t$  were calculated by the relationship  $N_t = 2 \times N_s \times \Delta C/C$ , with  $N_s$  being the effective doping concentration and  $\Delta C$  the amplitude of the capacitance transient.

### 3. Experimental results

The different observed peaks are labeled by the letter E or H with consecutive numbers for electron and hole traps respectively (e.g. see Fig. 1). Note that the peaks E5 and E8 consist of two levels and are therefore additionally labeled with the letters a and b (e.g. E5-a, E5-b). In cases where such a separation was not possible the results for E5 and E8 with omitted sublabelling are given for the superposition of both sublevels. The deconvolution of peak E8 was performed by a fitting procedure as shown in Ref. [9] while later on, during an isochronal heat treatment, the two components could also be measured directly (see below). The separation of peak E5 was done by varying the duration of the filling pulse making use of the level bistability (E5-a, E4) which is described in detail in Ref. [11].

#### 3.1. Neutron-irradiated samples

##### 3.1.1. Annealing at room temperature

The evolution of the DLTS spectrum within the first 160 h of annealing at room temperature (21°C) after neutron-irradiation is shown in Fig. 1. Typically 7 electron and 2 hole traps are observed, six of the corresponding peaks exhibiting a time dependence. The concentrations of E3 and H1 decrease while the ones of E5 and H2 grow. A fit to the data reveals that all four concentrations change exponentially with time constants around 80 h. Comparing the observed defect level parameters as given in Table 1 and the annealing time constants with those known from the literature [11–14], it is evident that the observed changes are due to the reactions:  $C_i(E3 \text{ and } H1) + C_s \rightarrow C_iC_s$  (E4 and E5-a) and  $C_i + O_i \rightarrow C_iO_i$  (H2). The level E1 was only seen during the first two weeks of room temperature annealing. Its concentration had grown within the first 24 h up to a fluence normalised value of  $0.1 \text{ cm}^{-1}$  and then annealed out within the following two weeks. Furthermore, a slight decrease of the peak E8 was observed with a time

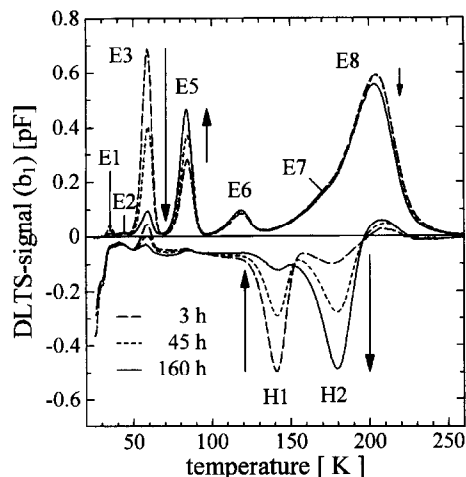


Fig. 1. Spectrum transformation at room temperature within 160 h after neutron-irradiation ( $\Phi = 2 \times 10^{11}$  n/cm<sup>2</sup>). The spectra were obtained with a time window of 200 ms and a filling pulse duration of 100 ms.

constant of about two weeks. The characteristic level parameters  $\Delta E_t$  and  $\sigma_t$  and the introduction rates  $g_t$  of all observed levels are given in Table 1 along with the most probable assignments to defects. It should be mentioned that it is not ensured that all hole traps are completely filled by hole injection in  $p^+n$ -diodes. This is obvious from the determined introduction rates of E3 and H1 which differ by a factor of 1.5 although the levels correspond to the electron and hole trap of the same defect ( $C_i$ ).

##### 3.1.2. Isochronal heat treatment

One detector, irradiated with  $6 \times 10^{11}$  n/cm<sup>2</sup> and stored for 6 months at room temperature, was studied in more detail using isochronal annealing. The temperature was increased from 353 to 633 K in 20 K steps each lasting 20 min. In between, two subsequent annealing steps a DLTS measurement was performed. As can be seen in Fig. 2, a strong reduction of the E8 peak amplitude was observed and up to 493 K this decrease was accompanied by a shift of the peak position to higher temperatures. After the 493 K step, the Arrhenius analysis of the remaining E8 peak results in defect parameters previously extracted from a fit for the E8-b level [9]. Thus, the transformation of the E8 peak in the temperature range up to 493 K can be attributed to the annealing of the E8-a level, as indicated by the open triangles in Fig. 2. However, a deconvolution of the E8 peak as measured before tempering into the E8-a and E8-b levels reveals that also 19% of the initial E8-b concentration anneals out during the heat treatment up to the 493 K step. With further increasing temperature the E8-b level drops even more and is almost completely annealed after

Table 1

Ionisation energies, cross sections, introduction rates and most probable assignments with defects for the levels found in the neutron irradiated samples.

Defect	$\Delta E_i$ (eV)	$\sigma_i$ (cm <sup>2</sup> )	Introduction rate $g_i$ (cm <sup>-1</sup> )	Identification	Comment
E1	-0.08	$2 \times 10^{-13}$	—	Unknown	Anneal in and out at RT
E2	-0.09	$6 \times 10^{-14}$	$\approx 0.03^a$	Unknown	
E3	-0.11	$6 \times 10^{-15}$	$1.5^b$	$C_i^{(-/0)}$	Anneal out at RT
E4	-0.11	$3 \times 10^{-15}$	—	$C_i C_s(B)^{(-/0)}$	Anneal in at RT
E5-a	-0.17	—	$0.38^a$	$C_i C_s(A)^{(-/0)}$	Anneal in at RT
E5-b	-0.17	$1 \times 10^{-14}$	$0.63^a$	$VO_i^{(-/0)}$	
E6	-0.24	$5 \times 10^{-15}$	$0.22^a$	$VV^{(-/-)}$	
E7	-0.37	$2 \times 10^{-14}$	$\approx 0.15^a$	Unknown	
E8-a	-0.39	$1 \times 10^{-15}$	$0.41^a$	Unknown	$\Delta E_i, \sigma_i, g_i$ extracted by fit
E8-b	-0.42	$1 \times 10^{-15}$	$0.71^a$	$VV^{(-/0)}$	$g_i$ extracted by fit
H1	+0.28	$4 \times 10^{-15}$	$1.0^b$	$C_i^{(+/0)}$	Anneal out at RT
H2	+0.36	$2 \times 10^{-15}$	$1.19^a$	$C_i O_i^{(+/0)}$	Anneal in at RT

Note: Defect parameters of the levels E6 and E7 could only be obtained by very long filling pulses ( $\approx 100$  ms) and are afflicted with a great uncertainty ( $\Delta E_i \approx 0.02$  eV and  $\Delta(\ln \sigma) \approx 1$ ) while the errors for the other levels are  $\Delta E_i < 0.01$  eV and  $\Delta(\ln \sigma) < 0.5$ . (a) Measured one month after irradiation. (b) Measured 1 h after irradiation.

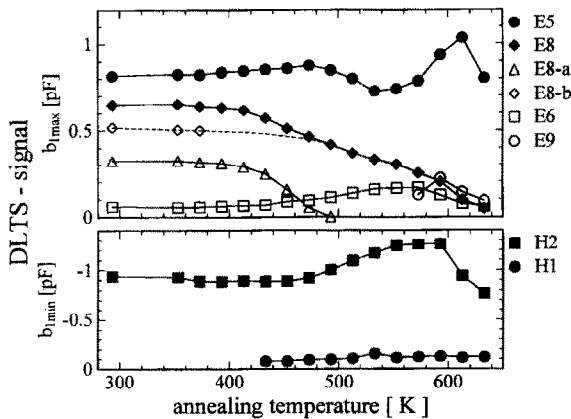


Fig. 2. Changes of the DLTS-peak heights of the various electron (upper part) and hole traps (lower part) during the isochronal heat treatment.

the last step at 633 K. This further reassures the assignment of the E8-b level to the singly charged divacancy  $VV^{(-/0)}$  (see Table 1 and 2) because this trap is known to have an annealing temperature of about 610 K [15]. Also the annealing behaviour of the other observed defects tally with the defect assignments given in Table 1 as can be seen in Table 2 where the annealing temperatures measured in this work are compared to the ones known from the literature. After the 573 K step a new level E9 was observed which annealed out again after the 633 K step. This annealing behaviour is consistent with that of a level attributed to the defect  $V_2O$  in Ref. [20]. How-

ever, the ionisation energy given for the level in Ref. [20] is 0.30 eV while the one measured in this work is 0.35 eV. Therefore, the assignment to  $V_2O$  is highly questionable and the origin of this defect remains unknown. It has to be noted that for the isochronal heat treatment the used filling pulse time of 1 ms was not sufficient for two traps to be filled completely in this high-resistivity material. The defect level E6 was only partly and E7 was almost not filled during the DLTS scans. Improved measurements with larger filling times and particular attention to the E8 peak are under way.

### 3.2. $^{60}Co$ -gamma irradiated samples

Four diodes were irradiated with  $^{60}Co$ -gammas in a dose range from 150 krad to 11 Mrad. The corresponding DLTS-spectra measured 3 months after irradiation are shown in Fig. 3. They were obtained using a time window of 20 ms and a filling pulse duration of 100 ms to completely fill all traps. During a DLTS measurement the E5 acceptor level is negatively charged below about 100 K and therefore compensates part of the positively charged shallow donors. For the heavily irradiated samples (at 3 and 11 Mrad) the concentration of level E5 was in the order of the shallow doping concentration. Hence, measurements below 100 K were not possible any more. This effect is also seen in the reduced peak amplitude of the E6 level observed on the sample irradiated with a dose of 11 Mrad and furthermore leads to a great uncertainty for the measured defect parameters of level E2.

Table 2

Comparison of the annealing temperatures observed in this work with the ones taken directly from the literature or calculated by the activation energies  $E_A$  and the frequency factors  $k_0$  given in the literature.

This work				Defect	Data taken from literature				
$\Delta E_i$ (eV)	$T_{\text{ann}}$ (K)		$\Delta E_i$ (eV)		$T_{\text{ann}}$ (K) Out	$k_0$ (s <sup>-1</sup> )	$E_A$ (eV)	Ref.	
	In	Out							
E5-a	- 0.17	≈ 300	533	C <sub>i</sub> C <sub>s</sub>	- 0.17	533	$2.5 \times 10^{13}$	1.70	[11, 16]
E5-b	- 0.17	-	> 633	VO <sub>i</sub>	- 0.18	633	$1.6 \times 10^{15}$	2.27	[17, 18]
E9	- 0.35	573	633	V <sub>2</sub> O(?)	- 0.30	570 ... 620	-	-	[19, 20]
E8-a	- 0.39	-	473	Unknown	-	-	-	-	-
E8-b	- 0.42	-	613	V <sub>2</sub>	- 0.41	613	$1.1 \times 10^9$	1.47	[15]
H2	+ 0.36	≈ 300	> 633	C <sub>i</sub> O <sub>i</sub>	+ 0.38	620 ... 670	-	-	[13, 21]

Note: The annealing temperature  $T_{\text{ann}}$  is defined as the temperature step at which the defect concentration drops below 1/e (37%) of the initial concentration.

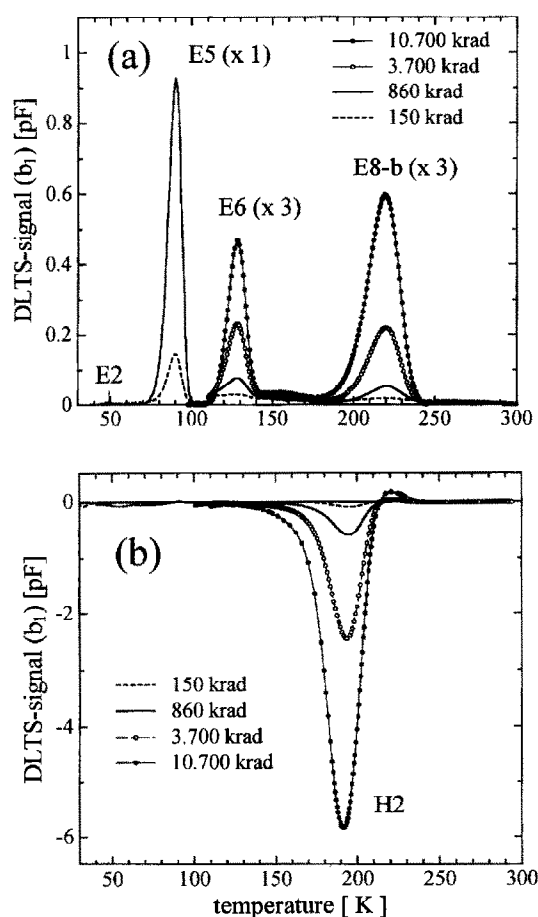


Fig. 3. DLTS-spectra after (a) electron and (b) hole injection of four samples irradiated with different <sup>60</sup>Co-gamma doses. Note that there are no data below 100 K for the heavily irradiated samples (dose > 1 Mrad) and that the peaks above 100 K in (a) are scaled by a factor of 3 for better visibility.

#### 4. Discussion

Comparing the spectra and the extracted defect parameters and introduction rates for the gamma-irradiated samples (Fig. 3, Table 3) with that for the neutron-irradiated ones (Fig. 1, Table 1) some differences become obvious. These differences have to be explained in terms of the primary defects, Vacancies (V) and Interstitials (I), produced by the PKA (Primary Knock on Atom). In gamma, respectively electron irradiations, the densities of the primary defects are very small compared to the densities that occur in neutron irradiations at the end of a PKA cascade. It is therefore assumed that neutrons produce far more divacancies and higher-order vacancy complexes in relation to other point defects than gammas. This actually is seen in this work by comparing e.g. the ratios of the production rates of the divacancy (VV) and the A-centre (VO<sub>i</sub>). For the gammas a ratio of 1 : 35 and for the neutrons a ratio of about 1 : 1 was found. Furthermore, taking into account that the effective sink for interstitials I is the reaction  $I + C_s \rightarrow C_i$  and that the C<sub>i</sub> later on end up in the defects C<sub>i</sub>C<sub>s</sub> and C<sub>i</sub>O<sub>i</sub> while the effective sink for the vacancies is the reaction  $V + O_i \rightarrow VO_i$  ending up in the A-centre (VO<sub>i</sub>), the ratio of  $([C_iC_s] + [C_iO_i]) : [VO_i]$  displays the ratio of diffusing interstitials to diffusing vacancies which escaped the primary recombination process. This ratio is 1 : 0.9 for the gammas and 1 : 0.4 for the neutrons also showing that in neutron irradiations far more vacancies are incorporated in divacancies, other vacancy related defects, and may be also clusters directly after the kick out reactions. Taking this into consideration most of the divacancies occur in lattice regions with a large lattice strain. According to a model of Svensson [22] lattice strain reduces the signal of the doubly charged divacancy in DLTS spectra which is in agreement with the deviation from the 1 : 1 ratio of the concentrations of singly and doubly charged

Table 3

Ionisation energies, cross sections, introduction rates and most probable assignments with defects for the levels found in the  $^{60}\text{Co}$ -gamma-irradiated samples measured three months after irradiation.

Defect	$\Delta E_i$ (eV)	$\sigma_i(\text{cm}^2)$	Introduction rate ( $10^3 \text{ cm}^{-3} \text{ rad}^{-1}$ )	Identification
E2	−0.09	—	$\approx 14$	Unknown
E4	−0.11	$2 \times 10^{-15}$	—	$\text{C}_i\text{C}_s(\text{B})^{(-/0)}$
E5-a	−0.17	—	130	$\text{C}_i\text{C}_s(\text{A})^{(-/0)}$
E5-b	−0.17	$1 \times 10^{-14}$	550	$\text{VO}_i^{(-/0)}$
E6	−0.22	$5 \times 10^{-16}$	15	$\text{VV}^{(-/-)}$
E8-b	−0.42	$2 \times 10^{-15}$	16	$\text{VV}^{(-/0)}$
H2	+0.36	$2 \times 10^{-15}$	460	$\text{C}_i\text{O}_i^{(+/0)}$

divacancies which was measured in this work for the neutron-irradiated samples.

In conclusion, one would expect that the two levels  $E_C - 0.39$  and  $-0.37$  eV, which were only observed in the neutron-irradiated samples, are related to higher-order vacancy defects, because most of the cluster models predict that interstitials migrate out of the primary damage regions while the vacancies stay and form the clusters [23]. However, comparing the number of the identified vacancy related defects to that of the identified interstitial ones ( $[\text{VO}_i] + 2 \times [\text{VV}]:([\text{C}_i\text{C}_s] + [\text{C}_i\text{O}_i])$ ) one gets a ratio of 1:1 for gamma irradiation but a ratio of 1:0.8 for neutrons. This suggests that at least one of these both levels is related to a higher-order interstitial related defect. Due to this contradictory statements the only characteristic feature of both defects that can be given in this work beside their level parameters and generation rates is that they are related to intrinsic defects of higher order and are produced close to or even in clusters.

## References

- [1] A. Chilingarov et al., Nucl. Instr. and Meth. A 360 (1995) 432 and literature cited there.
- [2] H. Feick et al., Nucl. Instr. and Meth. A 377 (1996) 217.
- [3] J. Matheson et al., RD20 Technical Report TN/36, 1995.
- [4] G. Lutz, MPI-Halbleiterlabor, München MPI-PhE/95-27.
- [5] G. Lutz, MPI-Halbleiterlabor, München; J. Kemmer, Ketek GmbH, München, private communication.
- [6] R. Schmidt et al., Med. Phys. 7 (1980) 507.
- [7] R. Wunstorff, Ph.D. Thesis, Universität Hamburg, see also DESY FH1K-92-01, 1992.
- [8] Dr. L. Cohausz, Halbleitermeßtechnik GmbH, Moosburg.
- [9] E. Fretwurst et al., Nucl. Instr. and Meth. A 377 (1996) 258.
- [10] S. Weiss, Ph.D. Thesis, University Kassel, 1991.
- [11] L.W. Song et al., Phys. Rev. B 42 (1990) 5765.
- [12] L.W. Song and G.D. Watkins, Phys. Rev. B 42 (1990) 5759.
- [13] J.M. Trombetta and G.D. Watkins, Appl. Phys. Lett. 51 (1987) 1103.
- [14] V. Eremin et al., IEEE Trans. Nucl. Sci. NS-42 (1995) 387.
- [15] A.O. Ewvaraye and E. Sun, J. Appl. Phys. 47 (1976) 3776.
- [16] G. Davies and K.T. Kun, Semicond. Sci. Technol. 4 (1989) 327.
- [17] B.G. Svensson and J.L. Lindström, Phys. Rev. B 34 (1986) 8709.
- [18] L.C. Kimerling, Inst. Phys. Conf. Ser. (31) (1977) 221.
- [19] Y.H. Lee and J.W. Corbett, Phys. Rev. B 6 (1976) 2653.
- [20] O.O. Awadelkarim et al., J. Appl. Phys. 60 (1986) 1974.
- [21] P.M. Mooney et al., Phys. Rev. B 15 (1977) 3836.
- [22] B.G. Svensson et al., Phys. Rev. B 43 (1991) 2292.
- [23] L.S. Smirnov, A Survey of Semiconductor Radiation Techniques (Mir Publishers, Moscow, 1983).